Published in final edited form as:
J Pathol. 2017 December ; 243(4): 442–456. doi:10.1002/path.4977.

PTEN loss and activation of K-RAS and β-catenin cooperate to accelerate prostate tumourigenesis

Matthew T. Jefferies[1,2,*], **Adam C. Cox**[1,3,*], **Boris Y. Shorning**[1], **Valerie Meniel**[1], **David Griffiths**[4], **Howard G. Kynaston**[2,5], **Matthew J. Smalley**[1,6], and **Alan R. Clarke**[1]

[1]The European Cancer Stem Cell Research Institute, School of Biosciences, Cardiff University, UK

[2]Institute of Cancer and Genetics, Cardiff University School of Medicine, Heath Park, Cardiff, UK

[3]Department of Urology, Morriston Hospital, Swansea, UK

[4]Department of Pathology, University Hospital of Wales, Cardiff, UK

[5]Department of Urology, University Hospital of Wales, Cardiff

Abstract

Aberrant phosphoinositide-3-kinase **(**PI3K), mitogen-activated protein kinase (MAPK) and WNT signalling are emerging as key events in the multistep nature of prostate tumourigenesis and progression. Here we report a compound prostate cancer murine model, in which these signalling pathways cooperate to produce a more aggressive prostate cancer phenotype. Using Cre-LoxP technology and the Probasin promoter, we combined the loss of *Pten* (*Pten*$^{fl/fl}$), to activate the PI3K signalling pathway, with dominant stabilised β-catenin (*Catnb*$^{+/lox(ex3)}$) and activated K-RAS (*K-Ras*$^{+/V12}$) to aberrantly activate WNT and MAPK signalling, respectively. Synchronous activation of all three pathways (triple mutant) significantly reduced survival (median 96 days) compared to double (median 140 days for *Catnb*$^{+/lox(ex3)}$*Pten*$^{fl/fl}$; 182 days for *Catnb*$^{+/lox(ex3)}$*K-Ras*$^{+/V12}$; 238 days for *Pten*$^{fl/fl}$*K-Ras*$^{+/V12}$) and single mutant mice (median 383 days for *Catnb*$^{+/lox(ex3)}$; 407 days for *Pten*$^{fl/fl}$), reflecting the accelerated tumourigenesis. Tumours followed a step-wise progression from mouse prostate intraepithelial neoplasia (mPIN) to invasive adenocarcinoma, similar to that seen in human disease. There was significantly elevated cellular proliferation, tumour growth and percentage of invasive adenocarcinoma in triple mutant mice compared to double and single mutants. Triple mutants not only displayed activated AKT, ERK1/2 and nuclear β-catenin but also significantly elevated mechanistic target of rapamycin complex 1 (mTORC1) signalling. In summary, we show that combined deregulation of the PI3K, MAPK and WNT signalling pathways drives rapid progression of prostate tumourigenesis, and that deregulation of all three pathways results in tumours showing aberrant mTORC1 signalling. As

[6]Corresponding author: The European Cancer Stem Cell Research Institute, School of Biosciences, Cardiff University, Hadyn Ellis Building, Maindy Road, Cardiff, CF24 4HQ, UK. Telephone: +44 (0)2920 875862. SmalleyMJ@cardiff.ac.uk.
*Authors made equal contributions.

Author contributions
Study concept and design: MTJ, ACC, HGK and ARC; study supervision: ARC and HGK; acquisition and analysis of data: all authors; drafting of manuscript: MTJ, BYS, ARC and MJS. All authors had final approval of the submitted and published version.

Conflicts of interest
None.

Europe PMC Funders Author Manuscripts

mTORC1 signalling is emerging as a key driver of androgen deprivation therapy resistance, our findings are important for understanding the biology of therapy-resistant prostate cancer and identifying potential approaches to overcome this.

Keywords

Prostate Cancer; *Pten*; *K-Ras*; *β-catenin*; WNT; mTORC1

Europe PMC Funders Author Manuscripts

Introduction

Advanced molecular and genetic technologies have identified a vast number of somatic mutations, copy number alterations, and oncogenic structural DNA rearrangements in both primary[1–5] and metastatic prostate cancer (PCa)[6–10]. However, these studies, together with the COSMIC database (http://cancer.sanger.ac.uk/cosmic), highlight a limited number of highly recurrent abnormalities in specific genes/pathways. Recurrent somatic mutations in cell signalling pathways or processes that can be clinically actionable/targeted by emerging therapies include for example the WNT, phosphoinositide-3-kinase **(**PI3K) and mitogen-activated protein kinase (MAPK) signalling pathways.

Deregulation of WNT signalling is implicated in many cancers. The best known example is colorectal cancer, where greater than 90% have an activating mutation of the canonical WNT signalling pathway [11]. In PCa, deregulated WNT signalling has been primarily investigated in metastatic disease, with somatic alteration of the Adenomatous Polyposis Coli tumour suppressor gene (*APC*) and β-catenin reported in 8.7-19.7% and 4.9-12% of cases, respectively[7,10]. WNT signalling has also been implicated in the lethal phase of PCa, castrate resistant prostate cancer (CRPC), independent of androgen signalling[6,7]. Up-regulation of the PI3K pathway, encompassing multiple somatic alterations such as deletion/mutations in PTEN, PI3K or AKT, has been reported in 42% of primary tumours and 100% of metastatic tumours[1] suggesting that this pathway plays a key role in the ability of the cancer cell to metastasise. Lastly, aberrations that result in the upregulation of the MAPK pathway are also common in PCa, with pathway alterations reported in 43% of primary tumours and 90% of metastasis[1]. Furthermore, the MAPK signalling pathway has not only been implicated in the initial phase of metastasis but also the late transition to CRPC[12].

Historically, signalling pathways have been studied as linear entities that do not interact; however the importance of pathway crosstalk which results in complex signalling webs is now understood. There is growing appreciation that this crosstalk is key for tumour development and progression. We have previously shown in the mouse that the WNT and MAPK pathways synergise to accelerate prostate tumourigenesis[13]. Others have demonstrated that canonical WNT signalling promotes prostate carcinogenesis driven by FGFR1 (which activates both PI3K and MEK/ERK pathways)[14]. The crosstalk between WNT and PI3K pathways in prostate tumourigenesis has been shown previously[15] and several studies have investigated synergistic effects between PI3K and MAPK pathways in mouse models[16–19]. Mechanisms of c-MYC activation also suggest a possible convergence between the WNT, PI3K and MAPK pathways in PCa. *c-Myc* is an important

WNT target gene and a key effector of deregulated WNT signalling[20] although can also be activated in a WNT-independent manner, as demonstrated in a murine PCa model of *Pten* deletion and mutant B-RAF activation[17].

We hypothesized that combined deregulation of PI3K, WNT and MAPK signalling would cooperate to accelerate prostate tumourigenesis. To test this, we used an *in vivo* genetics approach to combine aberrant PI3K, WNT and MAPK signalling in the mouse prostate[13]. We report here that while activating any two of these pathways together accelerates tumourigenesis over single pathway activation, combining all three further augments tumour formation, indicating each pathway makes a distinct contribution to the process of tumourigenesis. Furthermore, we observed strongest mTORC1 activation in triple mutants, consistent with findings from a human PCa tissue microarray, suggesting this may be the target of the synergistic activity of these three pathways. As mTORC1 signalling is emerging as a key driver of androgen deprivation therapy (ADT) resistance and stimulates tumour growth in the setting of castrate levels of testosterone, our findings are important for understanding the biology of therapy-resistant PCa and identifying potential approaches to overcome this.

Materials and Methods

Experimental animals

All animal studies and breeding were carried out under UK Home Office regulations following local ethical approval and according to the ARRIVE guidelines[21]. *Probasin (Pb)-Cre4* mice were sourced from the Mouse Models of Human Cancer Consortium (National Cancer Institute-Frederick). The alleles used in this study were β-*catenin*$^{+/lox(ex3)}$ [22], *K-Ras*$^{+/V12}$[23] and *Pten*$^{fl/fl}$[24]. The *Pb-Cre4* transgene was incorporated into cohorts using male mice, as *Pb-Cre4* positive female mice have been shown to recombine in the ovaries resulting in a mosaic phenotype[25]. Mice were genotyped from DNA isolated from ear nicks. Each *loxP*-targeted allele and the Cre-recombinase transgene were detected as described previously[22–24]. Kaplan–Meier survival analysis was carried out using GraphPad Prism (Version 5.0b). Only mice which reached specified endpoints when euthanasia was necessary due to prostate disease were included in KM curves.

In some cases, bromodeoxyuridine (BrdU, GE Healthcare, Buckinghamshire, UK) was administered via intra-peritoneal injection; mice were euthanized 2 hours post-administration.

Tissue isolation and histology

Tissue was harvested and fixed in 10% neutral buffered formaldehyde at 4°C for no more than 24 hours. Samples were embedded in paraffin and sectioned at 5μm and stained with haematoxylin and eosin (H&E) for histological analysis. To assess the severity or aggressiveness of the tumour histologically, the percentage of invasion was estimated at 100 days and end point (death or 500 days).

Histological analysis of the prostate gland was performed in accordance with the consensus report from the New York meeting of the Mouse Models of Human Cancer Consortium

prostate pathology committee[26]. The histological subtype descriptors used were mouse prostate intraepithelial neoplasia (mPIN), microinvasive adenocarcinoma and invasive adenocarcinoma.

Immunohistochemistry, tissue micro-array (TMA) analysis and Western blotting

Standard immunohistochemistry and western blotting techniques were used throughout this study. TMA prostate samples were approved under the Human Tissue Act (HTA) and WCB project number 12/007. Full details of the antibodies used and dilutions, staining quantitation methods ("Quickscore") and TMA analysis are provided in the Supplementary Material.

Results

WNT, PI3K and MAPK signalling are elevated in human PCa and are associated with mTORC1 pathway

A number of studies have suggested the importance of WNT, PI3K and MAPK signalling in initiation, progression and metastasis of human PCa[1,6,7,10–12] and tissue microarray analysis previously showed simultaneous activation of PI3K/AKT and RAS/MAPK signaling in patients with late-stage prostate disease[16–19]. To assess the interaction between these pathways and help identify a pathway of potential convergence, we analysed human PCa using a tissue microarray of 317 samples, 244 prostate adenocarcinomas and 73 benign controls (Welsh Cancer Bank). We found significant up-regulation of markers associated with activation of all three pathways (WNT, PI3K and MAPK signalling) in PCa when compared to benign controls (Fig.1A-C). Furthermore, when separating samples based on no/mild staining to moderate/strong staining for downstream mTORC1 marker p-S6, there was clear correlation between p-S6 staining and activation of all three pathways (Fig. 1D-E). Our data therefore suggested that mTORC1 signalling may act as a convergence point for these three pathways.

Pten loss and activation of K-Ras and β-catenin (triple mutants) cooperate to accelerate prostate tumourigenesis

To test the hypothesis that mTORC1 signalling in PCa requires simultaneous activation of WNT, PI3K and MAPK pathways, we used an *in vivo* genetics approach. We generated 8 cohorts of *Pb-Cre4* positive mice carrying different combinations of conditional alleles for *Pten* loss ($Pten^{fl/fl}$) and for β-catenin ($Catnb^{+/lox(ex3)}$) and K-RAS ($K\text{-}Ras^{+/V12}$) activation. These were subdivided into three groups according to their genotype: 4 "singles" (WT, $Pten^{fl/fl}$, $Catnb^{+/lox(ex3)}$ and $K\text{-}Ras^{+/V12}$), 3 "doubles" ($Catnb^{+/lox(ex3)}K\text{-}Ras^{+/V12}$, $Pten^{fl/fl}K\text{-}Ras^{+/V12}$, $Catnb^{+/lox(ex3)}Pten^{fl/fl}$) and a "triple" ($Catnb^{+/lox(ex3)}Pten^{fl/fl}K\text{-}Ras^{+/V12}$). 15 animals from each cohort were aged until they reached specified endpoints or 500 days, which ever was sooner. Additional mice were humanely killed for histological and western blotting analysis at 100 days (n=6) and at timepoints of 70, 100, 200, 250 ($Pten^{fl/fl}K\text{-}Ras^{+/V12}$ only), 300, 350 ($Pten^{fl/fl}$ only) and 400 days to weigh prostates in order to estimate increasing tumour burden over time (n=3).

All wild-type (WT) and *Pb-Cre4*$^{+}$*K-Ras*$^{+/V12}$ single mutant mice survived until the end of the experiment (500 days). As previously reported[13] and similar to *K-Ras*$^{+/D12}$ expressed alone[16–19] *K-Ras*$^{+/V12}$ mice did not produce PCa, with all mice surviving to the end of the experiment (500 days). All other mouse models developed extensive invasive adenocarcinoma of the prostate (100% incidence) resulting in ureteric or bladder outflow obstruction secondary to the local effects of the primary tumour. Consistent with reports from others[13,27], activation of β-catenin (*Pb-Cre4*$^{+}$*Catnb*$^{+/ex3}$) or homozygous deletion of *Pten* (*Pb-Cre4*$^{+}$*Pten*$^{fl/fl}$) resulted in a reduced median survival of 383 days (Range 339-476) and 407 days (Range 350-479) respectively (Fig.1F).

All double mutant mice had reduced survival when compared to single mutants ($p<0.0001$, Log-Rank) (Fig.1F). Mice with activation of both β-catenin and K-RAS (*Pb-Cre4*$^{+}$*Catnb*$^{+/ex3}$*K-Ras*$^{+/V12}$) had a median survival of 182 days (Range 170-208), as reported previously[13]. Mice with loss of *Pten* and activation of β-catenin (*Pb-Cre4*$^{+}$*Catnb*$^{+/ex3}$*Pten*$^{fl/fl}$) had a median survival of 140 days (Range 109-181). Mice with both *Pten* loss and activation of K-RAS (*Pb-Cre4*$^{+}$*Pten*$^{fl/fl}$*K-Ras*$^{+/V12}$) had median survival that was reduced to 238 days (Range 200-292, $p<0.0001$, Log-Rank; this is longer than in models using the more aggressive *K-Ras*$^{+/D12}$: 20 and 40 weeks median survival are reported for *Pten*$^{fl/fl}$*K-Ras*$^{+/D12}$ and *Pten*$^{+/fl}$*K-Ras*$^{+/D12}$ respectively)[16–19]. Compared to double mutants, however, triple mutant mice with *Pten* loss in addition to activation of β-catenin and K-RAS (*Pb-Cre4*$^{+}$*Catnb*$^{+/ex3}$*Pten*$^{fl/fl}$*K-Ras*$^{+/V12}$) demonstrated significantly earlier morbidity and mortality with a median survival of 96 days ($n = 15$; Range 76-130, $p<0.0001$, Log-Rank) (Fig.1F).

Tumour progression occurs in a stepwise fashion similar to that of human disease from mouse PIN (mPIN) to invasive adenocarcinoma

All tumour models examined demonstrated stepwise progression from mouse prostate intraepithelial neoplasia (mPIN) to microinvasive and invasive adenocarcinoma (Fig.2) as the cohorts aged (as shown by analysis of mice at day 70 – day 400 timepoints).

Histologically normal prostates from wild type (WT) mice (Fig.2A-C) showed avid androgen receptor (AR) staining of luminal epithelial cells as well as some stromal reactivity (Fig.2B) and had an intact basal layer confirmed by positive cytokeratin (CK) 5 staining (Fig.2C). mPIN was characterised by increased cell proliferation within the glands with frequent cellular atypia (Fig.2D). There was positive nuclear AR staining (Fig.2E) of the luminal cells and positive membranous CK5 staining of the basal layer (Fig.2F). Lesions were classified as microinvasive adenocarcinoma when the normal glandular structure showed distortions with some epithelial cells invading into the surrounding stroma (typically <1mm). At the site of such invasion there was a breach in the basal layer with local loss of basal cell marker CK5 but positive AR staining of the cells invading the stroma (Fig.2G-I). Similarly to human PCa, invasive adenocarcinoma of mouse prostate exhibited widespread loss of CK5 positivity and the whole basal layer was breached allowing invasion of epithelial cells into the stroma (Fig.2J-L and Supplementary Fig.S1A-C). Tumours were rapidly proliferating with frequent mitoses and rare apoptotic bodies (Supplementary Fig.S1A,B). As the tumours progressed, the prostate glandular architecture became

increasingly distorted as glands fused together and areas of cribriform pattern formed, pathognomonic of Gleason pattern 4 (Fig.2J & Supplementary Fig.S1B). Furthermore, features of Gleason pattern 5 developed; with single PCa cells appearing in the stroma (Supplementary Fig.S1C).

All tumour models investigated displayed reactive stroma and regions with mesenchymal morphology (spindle shaped cells that can be classified as sarcomatoid metaplasia) adjacent to epithelial areas with mPIN and invasive adenocarcinoma (Supplementary Fig.S1D). Abnormal differentiation was evident from regions staining for both epithelial (pan-cytokeratin, pCK) and mesenchymal (vimentin) IHC markers (Supplementary Fig.S1E,F).

In all models where a mutated β-catenin allele was present, squamous metaplasia characterised by epithelial-like tumour cells acquiring a squamous morphology and focal areas of hyperkeratinisation ('keratin pearls'; Supplementary Fig.S1G) was common, consistent with previous observations in mouse PCa models with activated WNT[13,15,28–31]. Areas of squamous metaplasia stained strongly for the basal keratin CK5 (Supplementary Fig.S1H), in contrast to prostate adenocarcinoma (Fig.2L).

Combinatorial pathway mutations shifts the spectrum of lesions to a more aggressive phenotype

To compare progression of disease between different mouse models, we assessed the percentage of invasive adenocarcinoma within each mouse cohort at a fixed timepoint of 100 days (Supplementary Fig.S2). As expected, WT and single *K-Ras*$^{+/V12}$ mutant mice had histologically normal prostates at this time. Single *Catnb*$^{+/ex3}$ and *Pten*$^{fl/fl}$ mice, and *Catnb*$^{+/lox(ex3)}$*K-Ras*$^{+/V12}$ mice, displayed areas of mPIN but no invasion at 100 days. *Pten*$^{fl/fl}$*K-Ras*$^{+/V12}$ *and Catnb*$^{+/lox(ex3)}$*Pten*$^{fl/fl}$ double mutant mice predominately showed mPIN with areas of microinvasive adenocarcinoma at 100 days (particularly the latter cohort), while triple mutants had widespread invasive adenocarcinoma. To assess the rate of growth of tumours, tumour burden was estimated by weighing prostates of mice killed at 70, 100, 200, 250 (*Pten*$^{fl/fl}$ *K-Ras*$^{+/V12}$ only), 300, 350 (for *Pten*$^{fl/fl}$ only) and 400 days (Supplementary Fig.S3). Prostate weights in *Catnb*$^{+/ex3}$*Pten*$^{fl/fl}$*K-Ras*$^{+/V12}$ triple mutants increased rapidly from the earliest timepoint; *Catnb*$^{+/lox(ex3)}$*Pten*$^{fl/fl}$ prostates showed a similar behaviour. The other cohorts either showed a delay before tumour growth or there was little or no increase in prostate weight at all (in the WT and *K-Ras*$^{+/V12}$ mice; Supplementary Fig.S3). These growth patterns were reflected by proliferation within tumours as analysed by Ki67 staining and BrdU labelling (Supplementary Fig.S4). Triple mutant mice had a significantly higher percentage of Ki67+ cells compared to all other genotypes at 100 days. By the experimental endpoint, proliferation in the triple mutants (by either Ki67 or BrdU) was still significantly higher than the WT and all the single mutant cohorts. However, proliferation in the double mutants at their endpoints was similar to that of the triple mutant mice at endpoint (the differences in proliferation at endpoint between *Pten*$^{fl/fl}$*K-Ras*$^{+/V12}$ and *Catnb*$^{+/ex3}$*Pten*$^{fl/fl}$*K-Ras*$^{+/V12}$ mice by Ki67 and between *Catnb*$^{+/lox(ex3)}$*Pten*$^{fl/fl}$ and *Catnb*$^{+/ex3}$*Pten*$^{fl/fl}$*K-Ras*$^{+/V12}$ mice by BrdU being not significant; Supplementary Fig.S4). The rate of apoptosis was low (<1%) across all tumours with no significant difference between genotypes (Supplementary Fig.S5).

Triple mutant mice therefore had faster growing tumours with a more aggressive histological phenotype and an increased amount of invasive adenocarcinoma resulting in significantly reduced survival when compared to double and single mutant mice.

Both K-Ras and β-catenin mutations drive metastatic spread in the context of loss of Pten

To assess metastatic potential in the mouse, retroperitoneal lymph nodes were harvested for each genotype and assessed histologically for metastasis (Fig.3). We observed metastatic deposits only in two cohorts: 10% (n=1/10) of *Catnb*$^{+/ex3}$*Pten*$^{fl/fl}$ and 60% (n=6/10) of *Pten*$^{fl/fl}$*K-Ras*$^{+/V12}$ double mutant mice demonstrated nodal metastasis (Supplementary Table S1). All metastatic lymph nodes examined had areas of neoplastic prostatic epithelium located at the capsule of the node, with fusion of glands and a cribriform pattern (Fig.3A), morphologically similar to that seen in the corresponding prostate tumour specimens and strongly positive for pan-cytokeratin (Fig.3B).

Triple mutation perturbs “checks and balances” of mTOR signalling regulation in mouse prostate

To assess whether the accelerated rate of tumour formation and rapid progression in the triple mutant mice was due to a synergistic effect between WNT, PI3K/AKT/mTOR and MAPK pathways, we assessed β-catenin levels and localisation, as well as key readouts of PI3K/AKT/mTOR and MAPK pathways, in prostate tissue of all cohorts by semi-quantitative immunohistochemistry on aged mice (Fig.4&5, Supplementary Fig.S6&S7) and western blot on 100 day old mice (Fig.6; Supplementary Fig.S8).

β-catenin localisation in aged mice was primarily at the cell membrane in prostates of WT, *Pten*$^{fl/fl}$, *K-Ras*$^{+/V12}$ and *Pten*$^{fl/fl}$*K-Ras*$^{+/V12}$ mutant mice (Fig.4A,D,J,M; Fig.5D), although some nuclear localisation was observed (Fig.4N). Nuclear localisation of β-catenin in *Pten*$^{fl/fl}$*K-Ras*$^{+/V12}$ mice was largely associated with invasive areas (Fig.5D) possibly due to relocalisation from cell membrane of invading cells after E-cadherin loss[32]. In single, double and triple mutant mice expressing *Catnb*$^{+/ex3}$, there was a significant increase in nuclear localisation of β-catenin (Fig.4G, N; Fig.5.A,G,J) but there was lower β-catenin nuclear staining in cohorts in which *Pten* had been knocked out but β-catenin was wild type (Fig.4N, Supplementary Table S2). Overall β-catenin levels as measured at 100 days were largely stable (Fig.6 and Supplementary Fig.S8), possibly due to negative feedback loops regulating WNT signalling[33,34], but in animals carrying a mutant *K-Ras*$^{+/V12}$ but β-catenin wild type, we observed a >2-fold decrease in total β-catenin levels (relative levels of β-catenin: WT=1, *K-Ras*$^{+/V12}$ = 0.44, $p<0.05$, *Pten*$^{fl/fl}$*K-Ras*$^{+/V12}$ = 0.43, p=0.05, Fig.6 and Supplementary Fig.S8).

AKT activation by phosphorylation at both regulatory residues was present at 100 days in all cohorts with *Pten* ablation and to a lesser extent in *Catnb*$^{+/ex3}$*K-Ras*$^{+/V12}$ mice (relative levels of p-AKT^{Thr308}: WT=1, *Pten*$^{fl/fl}$ =13.89, *Pten*$^{fl/fl}$*K-Ras*$^{+/V12}$ = 14.88, *Pten*$^{fl/fl}$*Catnb*$^{+/ex3}$ = 6.04; *Catnb*$^{+/ex3}$*K-Ras*$^{+/V12}$=1.89, *Catnb*$^{+/ex3}$*Pten*$^{fl/fl}$*K-Ras*$^{+/V12}$=7.62; p-AKT^{Ser473}: WT=1, *Pten*$^{fl/fl}$ =12.76, *Catnb*$^{+/ex3}$*K-Ras*$^{+/V12}$=2.90, *Catnb*$^{+/ex3}$*Pten*$^{fl/fl}$= 16.72, *Pten*$^{fl/fl}$*K-Ras*$^{+/V12}$=20.53, *Catnb*$^{+/ex3}$*Pten*$^{fl/fl}$*K-Ras*$^{+/V12}$= 9.36; for all comparisons $p<0.01$ relative to

WT; Fig.6 and Supplementary Fig.S8). This was confirmed by p-AKT^{Thr308} staining of aged prostates (Fig.4B,E,H,K and Fig.5B,E,H,K,M; SuppTable 1).

AKT is known to inhibit GSK3β activity by phosphorylating Ser9 residue[35], which can serve as readout of AKT activity. Although GSK3β is a part of β-catenin destruction complex, AKT-dependent Ser9 phosphorylation is not likely to affect WNT signalling, but rather TSC1/2[36]. Phospho-GSK3β^{Ser9} levels in prostates from aged mice (Supplementary Fig.S6) largely correlated with AKT activation, with staining detected only in cohorts with deleted *Pten* and in *Catnb*$^{+/ex3}$*K-Ras*$^{+/V12}$ mice (Supplementary Fig.S6). Prostates from the *Catnb*$^{+/ex3}$*Pten*$^{fl/fl}$ and *Catnb*$^{+/ex3}$*Pten*$^{fl/fl}$*K-Ras*$^{+/V12}$ cohorts had significantly higher levels of p-GSK3β^{Ser9} compared to all other cohorts (Supplementary Fig.S6H,I).

Total levels of p-ERK1/2 (p44/42 MAPK) were lower in 100 day old *K-Ras*$^{+/V12}$ mice and all other tumour models when compared with age matched WT animals by western blot (WT=1, *K-Ras*$^{+/V12}$=0.27, p<0.01, Fig.6 and Supplementary Fig.S8). Although these findings are surprising at face value, the ERK-signalling network has numerous negative feedback loops[37] and when *Pten* was deleted and β-catenin activated, *K-Ras*$^{+/V12}$ expression led to a 7.2-fold increase in p-ERK1/2 levels (*Catnb*$^{+/ex3}$*Pten*$^{fl/fl}$*K-Ras*$^{+/V12}$ vs *Catnb*$^{+/ex3}$*Pten*$^{fl/fl}$, p<0.01, Fig.6 and Supplementary Fig.S8), although this still did not fully rescue WT levels. However, immunostaining of aged prostates for p-ERK1/2 revealed that while WT mice tended to have moderate, uniform staining, tumour models were more heterogeneous with areas of focal strong staining which cannot be distinguished in western blot (Supplementary Fig.S7). Indeed, by Quickscore, aged WT and *K-Ras*$^{+/V12}$ mice had similar levels of p-ERK1/2 and all other models had significantly higher p-ERK1/2 levels (Supplementary Fig.S7I).

Finally, ribosomal protein S6 phosphorylation is a key readout of mTORC1 activity[38]. Western blot analysis of younger (100 day old) mice revealed that only the triple *Catnb*$^{+/ex3}$*Pten*$^{fl/fl}$*K-Ras*$^{+/V12}$ mice showed significantly increased levels of p-S6$^{240-244}$ (WT=1, *Catnb*$^{+/ex3}$*K-Ras*$^{+/V12}$ = 0.49, *Catnb*$^{+/ex3}$*Pten*$^{fl/fl}$ = 0.69, *Pten*$^{fl/fl}$*K-Ras*$^{+/V12}$ = 0.47, *Catnb*$^{+/ex3}$*Pten*$^{fl/fl}$*K-Ras*$^{+/V12}$ = 2.09, p<0.01; Fig.6 and Supplementary Fig.S8). This 3-4-fold increase in p-S6$^{240-244}$ levels observed in the triple compared to the double mutant mice suggests the abrogation of negative feedback loops controlling mTORC1. Furthermore, prostate tissue from aged *Catnb*$^{+/ex3}$*Pten*$^{fl/fl}$*K-Ras*$^{+/V12}$ mice also had significantly higher levels of p-S6$^{240-244}$ compared to aged mice of other genotypes (p<0.05 compared to the next closest genotype; Fig.4C,F,I,L, Fig.5C,F,I,L,N).

Therefore, our study supports the hypothesis that mTORC1 signalling in PCa requires simultaneous activation of WNT, PI3K and MAPK pathways, as suggested by the human TMA data, and that this results in a more aggressive tumour phenotype. Furthermore, it suggests that the parallel activation of WNT, PI3K/AKT/mTOR and MAPK signalling has its synergistic effect due to relieving multiple negative feedback loops and cross-talks between the pathways.

Discussion

Although the androgen signalling pathway and ADT are pivotal in the treatment of advanced PCa, men still relapse with CRPC. Given the importance of feedback within signaling networks, it is important to understand the potential outcomes of cross-talk between key signaling modules within the prostate and possible implications for CRPC. For example, androgen depletion leads to PI3K/AKT pathway stimulation[39] and increased nuclear co-localization and interaction of endogenous AR and β-catenin[40]. Our study provides evidence of clear synergistic crosstalk between the WNT, PI3K/AKT and MAPK signalling pathways driving progression in prostate tumourigenesis.

Transcriptional alterations in both PI3K/AKT and MAPK are common in PCa, particularly in metastatic tumours[1]. These two pathways are regulated by a number of cross-talks including both activating and inhibitory loops[41]. RAS can directly bind to and activate PI3K[42]. The TSC1/2 complex, a key suppressor of PI3K-dependent stimulation of mTOR[43], can be inhibited by oncogenic MAPK signalling through both ERK and ribosomal S6 kinase (RSK)-dependent phosphorylation, resulting in increased mTORC1 signalling[44]. Furthermore, both ERK[44] and RSK [45,46] have been shown to directly phosphorylate Raptor to enhance mTORC1 activity. AKT negatively regulates ERK activation by phosphorylating inhibitory sites in the RAF N-terminus[47], ERK phosphorylation inhibits RAF and MEK[48] and phosphorylation of the downstream mTORC1 effector S6K feeds back to inhibit AKT activity and in turn mTORC1 signalling[49]. mTORC1 inhibition in turn activates MAPK signalling through a PI3K-dependent feedback loop[50]. We illustrate the multitude of regulatory links between PI3K/AKT and MAPK in Supplementary Fig.S9.

Complex interactions between androgen depletion, PI3K/AKT/mTOR and MAPK pathways have therapeutic implications. mTORC1 signalling is emerging as a key pathway that directs ADT resistance and stimulates tumour growth in the setting of castrate levels of testosterone (CRPC)[51]. The importance of mTORC1 signalling has resulted in the development of inhibitors such as rapamycin and its analogues, including everolimus and temsirolimus. Early studies with these inhibitors in PCa demonstrated regression of PIN lesions in a mouse model overexpressing AKT[52] and inhibition of growth of xenograft models derived from human cells lines with *Pten* loss[53]. Despite these promising preclinical results and the success of mTORC1 inhibitors in the treatment of patients with metastatic renal cell carcinoma[54], the clinical use of mTORC1 inhibitors in men with metastatic PCa has been disappointing. Phase I/II trials using single agent such as rapamycin or everolimus, have failed to show anti-tumour effects with little response in PSA or clinical progression[55,56]. The lack of therapeutic effects can be ascribed to MAPK pathway activation through a PI3K-dependent feedback loop in prostate tumours of patients treated with mTOR inhibitors[50]. Dual PI3K/mTORC1/2 drugs such as BEZ235 (Novartis) have shown positive effects in overcoming Docetaxel resistance in pre-clinical studies[57] and in mouse xenograft models[58]. Although BEZ235 has been discontinued in PCa, the results have stimulated a search for agents targeting PI3K/AKT/mTOR signalling with more favourable therapeutic index[59].

WNT signalling can integrate with both the PI3K/AKT/mTOR and MAPK pathways either directly via the GSK-3β-TSC2 axis or indirectly via β-catenin-dependent canonical WNT signalling, stimulation of *c-Myc* transcription and inhibition of MAPK-stimulated senescence pathways (Supplemental Fig.S9)[60,61] or through β-catenin interactions with AR[40]. In the absence of a WNT signal, GSK-3β phosphorylates β-catenin as part of the destruction complex. When WNT signalling is activated, GSK-3β is sequestrated in multivesicular endosomes allowing β-catenin to accumulate[62]. GSK-3β can also phosphorylate TSC2 and promote TSC1/2 activity, therefore, WNT-dependent inhibition of GSK3β may stimulate mTOR signalling as well as canonical WNT pathway activation[60].

Furthermore, phosphorylation of GSKβ by AKT or ERK can also result in TSC1/2 activation[36] or β-catenin–dependent WNT signalling[61], respectively. GSKβ is known to interact with p53[63] and p53 is implicated in negative feedback loops controlling cell growth through restraining WNT signalling[34]. In some models, *Pten*-deficient mouse prostates exhibit activated p53 and senescence[64] and the RAS/RAF axis also can stimulate p16/p21/p53-dependent senescence in a variety of tissues[65]. Consistent with the convergence of these three pathways on mTORC1, and feedback loops and cross-talks regulating them, only simultaneous deregulation of the PI3K, WNT and MAPK pathways resulted in significantly elevated mTORC1 signalling in our mouse models.

Importantly, in our models, canonical WNT signalling was activated at the level of β-catenin, not further up the pathway, for instance by deletion of APC[30,66]. Collapse of the β-catenin destruction complex following APC loss will not only lead to β-catenin stabilisation but may also free GSK-3β to phosphorylate targets such as TSC2. In our system the presence of an activated β-catenin was sufficient to drive synergistic crosstalk with the PI3K/AKT and MAPK pathways. This has allowed us to isolate the specific role of β-catenin transcriptional activity.

Our findings are consistent with previous studies using similar animal models with single or double conditional alleles. However, we do see some differences. Some authors have reported senescence in models in which *Pten* alone was knocked-out in a prostate-specific manner[18,64], however, this is not true of all models[15] and we did not observe this. The differences may be due to background strain or the particular conditional allele being used. As previous authors reported[15], combined β-catenin activation and *Pten* deletion led to accelerated tumour growth, increased invasive ability and squamous differentiation. We found one incidence of metastasis with this combination, unlike a previous study which had no indication of metastases[15] but which culled mice at an earlier age than in our study. Activated β-catenin is likely to drive proliferation of invading cells and primary tumour growth but not metastasis as such, leading to death from primary tumour morbidity. The one $Catnb^{+/ex3}Pten^{fl/fl}$ mouse showing a metastasis is likely to have resulted from chance combination of rapid invasion of tumour cells with a longer lifespan.

We observed greater metastatic incidence in the $Pten^{fl/fl}K\text{-}Ras^{+/V12}$ model than in $Catnb^{+/ex3}Pten^{fl/fl}$ mice. $Pten^{fl/fl}K\text{-}Ras^{+/V12}$ mice had a longer survival than the more aggressive $Pten^{fl/fl}K\text{-}Ras^{+/D12}$ model described previously[16], but consistent with our findings macrometastatic lesions were reported in all $Pten^{fl/fl}K\text{-}Ras^{+/D12}$ and $Pten^{fl/+}K\text{-}Ras^{+/D12}$

mice. The more extensive nature of the metastases and their rapid development is likely to result from the use of the more aggressive *K-Ras*$^{+/D12}$ allele. Interestingly, some evidence of the presence of recombined alleles was detected in bone, but overt bone metastasis were not observed[16]. In a PCa model in which *Cre* was driven from a knock-in to the *Nkx3.1* promoter, the combination of BRAF^{V600E} activation with *Pten* deletion resulted in animal lethality comparable to *Pten*$^{fl/fl}$*K-Ras*$^{+/D12}$, with an extensive metastatic burden and was associated with elevated c-MYC activity[17]. In contrast to both our observations on *K-Ras*$^{+/V12}$ and previous data on *K-Ras*$^{+/D12}$[16], activation of BRAF^{V600E} alone stimulated cell proliferation[17]. Importantly, however, NKX3.1 is a negative regulator of c-MYC transcriptional activity, and the *Nkx3.1-Cre* knock-in has a haplo-insufficient phenotype with elevated basal levels of c-MYC activity[67]. Analysis of this model is therefore confounded by use of the the *Nkx3.1-Cre* knock-in and the role of c-MYC, which may be mimicking, at least partly, an activated β-catenin. Nevertheless, although mutant BRAF and KRAS belong to the same signalling axis, the differences between the models suggest their activation has different implications, particularly for proliferation. Taken together, these studies imply a distinct role for KRAS activation combined with *Pten* deletion in promoting prostate metastasis. It is likely that reason we did not observed metastasis in our triple mutant model is simply that the animals succumbed so rapidly to the growth of the primary tumour.

This study has limitations. The differences in prostate anatomy between mouse and human mean that the interactions of mouse prostate tissue with the microenvironment may be different between the species (and indeed different in different lobes), affecting neoplastic processes. More importantly, the main cause of death in human PCa is metastasis, typically to the bone, whereas mouse models of PCa need to the euthanased as a result of locally advanced tumours. Indeed, despite increased PI3K, WNT, MAPK and mTORC1 signalling, triple mutant mice did not develop lymph node metastasis. This is likely due to the rapid progression of the primary tumour not allowing necessary time for metastasis to develop. One model, *Pten*$^{fl/fl}$*K-Ras*$^{+/V12}$, did develop lymph node metastases in >50% of animals, consistent with previous reports[16]. However, they still had to be euthanased as a result of locally advanced prostate tumours. It is unclear whether, even in the models which show lymph node metastasis, dissemination to organs or bone would ever happen. There are few autochthonous mouse models of any cancer driven by genetic lesions mimicking human disease which spontaneously develop overt bone metastases, although SV40 T-antigen models can do so[68] and in *Pten*$^{fl/fl}$*K-Ras*$^{+/D12}$ mice recombined cells were detected in bone[16]. Therefore, there remains a lack of mouse models that truly mimic advanced PCa.

In summary, we show that the PI3K, WNT and MAPK signalling pathways co-operate to accelerate prostate tumourigenesis and activate mTORC1 signalling, one of the key drivers of resistance to ADT. Our findings suggest that in addition to PI3K pathway inhibition, AR inhibitors could be combined with either MAPK or WNT pathway inhibitors with therapeutic benefit in CRPC. However, although mTORC1 may be difficult to activate as a result of dysregulation of a single pathway, once activated it may require intervention of more than one pathway to inhibit its activity, or, indeed, to prevent feedback loops from activating other oncogenic pathways[50]. Our triple mutant mouse model provides an excellent system for pre-clinical studies of multiple pathway inhibition as a therapeutic approach to targeting mTOR.

Supplementary Material

Refer to Web version on PubMed Central for supplementary material.

Acknowledgements

This work was funded by Prostate Cancer UK (PG12-16). BYS is supported by the Prostate Cancer Research Centre and the European Cancer Stem Cell Research Institute. VM is supported by Cancer Research Wales. MJS is supported by Cancer Research UK. The authors would like to thank Dr Andrew Tee for his critical reading of the manuscript. This manuscript is dedicated to the memory of the late Alan Clarke.

References

1. Taylor BS, Schultz N, Hieronymus H, et al. Integrative genomic profiling of human prostate cancer. Cancer Cell. 2010; 18:11–22. [PubMed: 20579941]
2. Berger MF, Lawrence MS, Demichelis F, et al. The genomic complexity of primary human prostate cancer. Nature. 2011; 470:214–20. [PubMed: 21307934]
3. Barbieri CE, Baca SC, Lawrence MS, et al. Exome sequencing identifies recurrent SPOP, FOXA1 and MED12 mutations in prostate cancer. Nature Research. 2012; 44:685–9.
4. Baca SC, Prandi D, Lawrence MS, et al. Punctuated evolution of prostate cancer genomes. Cell. 2013; 153:666–77. [PubMed: 23622249]
5. Tomlins SA, Rhodes DR, Perner S, et al. Recurrent fusion of TMPRSS2 and ETS transcription factor genes in prostate cancer. Science. 2005; 310:644–8. [PubMed: 16254181]
6. Kumar A, White TA, MacKenzie AP, et al. Exome sequencing identifies a spectrum of mutation frequencies in advanced and lethal prostate cancers. Proc Natl Acad Sci USA. 2011; 108:17087–92. [PubMed: 21949389]
7. Grasso CS, Wu Y-M, Robinson DR, et al. The mutational landscape of lethal castration-resistant prostate cancer. Nature. 2012; 487:239–43. [PubMed: 22722839]
8. Rajan P, Sudbery IM, Villasevil MEM, et al. Next-generation sequencing of advanced prostate cancer treated with androgen-deprivation therapy. Eur Urol. 2014; 66:32–9. [PubMed: 24054872]
9. Beltran H, Yelensky R, Frampton GM, et al. Targeted next-generation sequencing of advanced prostate cancer identifies potential therapeutic targets and disease heterogeneity. Eur Urol. 2013; 63:920–6. [PubMed: 22981675]
10. Robinson D, Van Allen EM, Wu Y-M, et al. Integrative clinical genomics of advanced prostate cancer. Cell. 2015; 161:1215–28. [PubMed: 26000489]
11. Giles RH, van Es JH, Clevers H. Caught up in a Wnt storm: Wnt signaling in cancer. Biochim Biophys Acta. 2003; 1653:1–24. [PubMed: 12781368]
12. Mukherjee R, McGuinness DH, McCall P, et al. Upregulation of MAPK pathway is associated with survival in castrate-resistant prostate cancer. Br J Cancer. 2011; 104:1920–8. [PubMed: 21559022]
13. Pearson HB, Phesse TJ, Clarke AR. K-ras and Wnt signaling synergize to accelerate prostate tumorigenesis in the mouse. Cancer Res. 2009; 69:94–101. [PubMed: 19117991]
14. Carstens JL, Shahi P, Van Tsang S, et al. FGFR1-WNT-TGF-β signaling in prostate cancer mouse models recapitulates human reactive stroma. Cancer Res. 2014; 74:609–20. [PubMed: 24305876]
15. Francis JC, Thomsen MK, Taketo MM, et al. Clurman BE. β-catenin is required for prostate development and cooperates with Pten loss to drive invasive carcinoma. PLoS Genet. 2013; 9:e1003180. [PubMed: 23300485]
16. Mulholland DJ, Kobayashi N, Ruscetti M, et al. Pten loss and RAS/MAPK activation cooperate to promote EMT and metastasis initiated from prostate cancer stem/progenitor cells. Cancer Res. 2012; 72:1878–89. [PubMed: 22350410]
17. Wang J, Kobayashi T, Floc'h N, et al. B-Raf activation cooperates with PTEN loss to drive c-Myc expression in advanced prostate cancer. Cancer Res. 2012; 72:4765–76. [PubMed: 22836754]
18. Ahmad I, Patel R, Singh LB, et al. HER2 overcomes PTEN (loss)-induced senescence to cause aggressive prostate cancer. Proc Natl Acad Sci USA. 2011; 108:16392–7. [PubMed: 21930937]

19. Patel R, Gao M, Ahmad I, et al. Sprouty2, PTEN, and PP2A interact to regulate prostate cancer progression. J Clin Invest. 2013; 123:1157–75. [PubMed: 23434594]
20. Sansom OJ, Meniel VS, Muncan V, et al. Myc deletion rescues Apc deficiency in the small intestine. Nature. 2007; 446:676–9. [PubMed: 17377531]
21. Kilkenny C, Browne WJ, Cuthill IC, et al. Improving bioscience research reporting: the ARRIVE guidelines for reporting animal research. PLoS biology. 2010; 8:e1000412. [PubMed: 20613859]
22. Harada N, Tamai Y, Ishikawa T, et al. Intestinal polyposis in mice with a dominant stable mutation of the beta-catenin gene. EMBO J. 1999; 18:5931–42. [PubMed: 10545105]
23. Guerra C, Mijimolle N, Dhawahir A, et al. Tumor induction by an endogenous K-ras oncogene is highly dependent on cellular context. Cancer Cell. 2003; 4:111–20. [PubMed: 12957286]
24. Suzuki A, Yamaguchi MT, Ohteki T, et al. T cell-specific loss of Pten leads to defects in central and peripheral tolerance. Immunity. 2001; 14:523–34. [PubMed: 11371355]
25. Wu X, Wu J, Huang J, et al. Generation of a prostate epithelial cell-specific Cre transgenic mouse model for tissue-specific gene ablation. Mech Dev. 2001; 101:61–9. [PubMed: 11231059]
26. Ittmann M, Huang J, Radaelli, et al. Animal models of human prostate cancer: The Consensus Report of the New York Meeting of the Mouse Models of Human Cancers Consortium Prostate Pathology Committee. Cancer Res. 2013; 73:2718–2736. [PubMed: 23610450]
27. Wang S, Gao J, Lei Q, et al. Prostate-specific deletion of the murine Pten tumor suppressor gene leads to metastatic prostate cancer. Cancer Cell. 2003; 4:209–21. [PubMed: 14522255]
28. Gounari F, Signoretti S, Bronson R, et al. Stabilization of beta-catenin induces lesions reminiscent of prostatic intraepithelial neoplasia, but terminal squamous transdifferentiation of other secretory epithelia. Oncogene. 2002; 21:4099–107. [PubMed: 12037666]
29. Bierie B, Nozawa M, Renou J-P, et al. Activation of beta-catenin in prostate epithelium induces hyperplasias and squamous transdifferentiation. Oncogene. 2003; 22:3875–87. [PubMed: 12813461]
30. Bruxvoort KJ, Charbonneau HM, Giambernardi TA, et al. Inactivation of Apc in the mouse prostate causes prostate carcinoma. Cancer Res. 2007; 67:2490–6. [PubMed: 17363566]
31. Bjerke GA, Pietrzak K, Melhuish TA, et al. Lau KM. Prostate cancer induced by loss of Apc is restrained by TGFβ signaling. PLoS ONE. 2014; 9:e92800. [PubMed: 24651496]
32. Orsulic S, Huber O, Aberle H, et al. E-cadherin binding prevents beta-catenin nuclear localization and beta-catenin/LEF-1-mediated transactivation. J Cell Sci. 1999; 112:1237–45. [PubMed: 10085258]
33. Reed KR, Meniel VS, Marsh V, et al. A limited role for p53 in modulating the immediate phenotype of Apc loss in the intestine. BMC Cancer. 2008; 8:162. [PubMed: 18533991]
34. Kim NH, Kim HS, Kim N-G, et al. p53 and microRNA-34 are suppressors of canonical Wnt signaling. Sci Signal. 2011; 4:71–1.
35. Cross DA, Alessi DR, Cohen P, et al. Inhibition of glycogen synthase kinase-3 by insulin mediated by protein kinase B. Nature. 1995; 378:785–9. [PubMed: 8524413]
36. McManus EJ, Sakamoto K, Armit LJ, et al. Role that phosphorylation of GSK3 plays in insulin and Wnt signalling defined by knockin analysis. EMBO J. 2005; 24:1571–83. [PubMed: 15791206]
37. Cirit M, Wang C-C, Haugh JM. Systematic quantification of negative feedback mechanisms in the extracellular signal-regulated kinase (ERK) signaling network. J Biol Chem. 2010; 285:36736–44. [PubMed: 20847054]
38. Ruvinsky I, Sharon N, Lerer T, et al. Ribosomal protein S6 phosphorylation is a determinant of cell size and glucose homeostasis. Genes Dev. 2005; 19:2199–211. [PubMed: 16166381]
39. Carver BS, Chapinski C, Wongvipat J, et al. Reciprocal feedback regulation of PI3K and androgen receptor signaling in PTEN-deficient prostate cancer. Cancer Cell. 2011; 19:575–86. [PubMed: 21575859]
40. Wang G, Wang J, Sadar MD. Crosstalk between the androgen receptor and beta-catenin in castrate-resistant prostate cancer. Cancer Res. 2008; 68:9918–27. [PubMed: 19047173]
41. Mendoza MC, Er EE, Blenis J. The Ras-ERK and PI3K-mTOR pathways: cross-talk and compensation. Trends Biochem Sci. 2011; 36:320–8. [PubMed: 21531565]

42. Suire S, Hawkins P, Stephens L. Activation of phosphoinositide 3-kinase gamma by Ras. Curr Biol. 2002; 12:1068–75. [PubMed: 12121613]
43. Manning BD, Tee AR, Logsdon MN, et al. Identification of the tuberous sclerosis complex-2 tumor suppressor gene product tuberin as a target of the phosphoinositide 3-kinase/akt pathway. Mol Cell. 2002; 10:151–62. [PubMed: 12150915]
44. Carriere A, Romeo Y, Acosta-Jaquez HA, et al. ERK1/2 phosphorylate Raptor to promote Ras-dependent activation of mTOR complex 1 (mTORC1). J Biol Chem. 2011; 286:567–77. [PubMed: 21071439]
45. Roux PP, Ballif BA, Anjum R, et al. Tumor-promoting phorbol esters and activated Ras inactivate the tuberous sclerosis tumor suppressor complex via p90 ribosomal S6 kinase. Proc Natl Acad Sci USA. 2004; 101:13489–94. [PubMed: 15342917]
46. Carriere A, Cargnello M, Julien L-A, et al. Oncogenic MAPK signaling stimulates mTORC1 activity by promoting RSK-mediated raptor phosphorylation. Curr Biol. 2008; 18:1269–77. [PubMed: 18722121]
47. Zimmermann S, Moelling K. Phosphorylation and regulation of Raf by Akt (protein kinase B). Science. 1999; 286:1741–4. [PubMed: 10576742]
48. Dhillon AS, Hagan S, Rath O, et al. MAP kinase signalling pathways in cancer. Oncogene. 2007; 26:3279–90. [PubMed: 17496922]
49. Dibble CC, Asara JM, Manning BD. Characterization of Rictor phosphorylation sites reveals direct regulation of mTOR complex 2 by S6K1. Mol Cell Biol. 2009; 29:5657–70. [PubMed: 19720745]
50. Carracedo A, Ma L, Teruya-Feldstein J, et al. Inhibition of mTORC1 leads to MAPK pathway activation through a PI3K-dependent feedback loop in human cancer. J Clin Invest. 2008; 118:3065–74. [PubMed: 18725988]
51. Edlind MP, Hsieh AC. PI3K-AKT-mTOR signaling in prostate cancer progression and androgen deprivation therapy resistance. Asian J Androl. 2014; 16:378–86. [PubMed: 24759575]
52. Majumder PK, Febbo PG, Bikoff R, et al. mTOR inhibition reverses Akt-dependent prostate intraepithelial neoplasia through regulation of apoptotic and HIF-1-dependent pathways. Nat Med. 2004; 10:594–601. [PubMed: 15156201]
53. Wu L, Birle DC, Tannock IF. Effects of the mammalian target of rapamycin inhibitor CCI-779 used alone or with chemotherapy on human prostate cancer cells and xenografts. Cancer Res. 2005; 65:2825–31. [PubMed: 15805283]
54. Motzer RJ, Escudier B, Oudard S, et al. Efficacy of everolimus in advanced renal cell carcinoma: a double-blind, randomised, placebo-controlled phase III trial. Lancet. 2008; 372:449–56. [PubMed: 18653228]
55. Templeton AJ, Dutoit V, Cathomas R, et al. Phase 2 trial of single-agent everolimus in chemotherapy-naive patients with castration-resistant prostate cancer (SAKK 08/08). Eur Urol. 2013; 64:150–8. [PubMed: 23582881]
56. Amato RJ, Jac J, Mohammad T, et al. Pilot study of rapamycin in patients with hormone-refractory prostate cancer. Clin Genitourin Cancer. 2008; 6:97–102. [PubMed: 18824432]
57. Antonarakis ES, Armstrong AJ. Evolving standards in the treatment of docetaxel-refractory castration-resistant prostate cancer. Prostate Cancer Prostatic Dis. 2011; 14:192–205. [PubMed: 21577234]
58. Yasumizu Y, Miyajima A, Kosaka T, et al. Dual PI3K/mTOR inhibitor NVP-BEZ235 sensitizes docetaxel in castration resistant prostate cancer. J Urol. 2014; 191:227–34. [PubMed: 23954373]
59. Wei XX, Hsieh AC, Kim W, et al. A Phase I Study of Abiraterone Acetate Combined with BEZ235, a Dual PI3K/mTOR Inhibitor, in Metastatic Castration Resistant Prostate Cancer. Oncologist. 2017; 22:503–43. [PubMed: 28314838]
60. Inoki K, Ouyang H, Zhu T, et al. TSC2 integrates Wnt and energy signals via a coordinated phosphorylation by AMPK and GSK3 to regulate cell growth. Cell. 2006; 126:955–68. [PubMed: 16959574]
61. Ding Q, Xia W, Liu J-C, et al. Erk associates with and primes GSK-3beta for its inactivation resulting in upregulation of beta-catenin. Mol Cell. 2005; 19:159–70. [PubMed: 16039586]

62. Taelman VF, Dobrowolski R, Plouhinec J-L, et al. Wnt signaling requires sequestration of glycogen synthase kinase 3 inside multivesicular endosomes. Cell. 2010; 143:1136–48. [PubMed: 21183076]

63. Watcharasit P, Bijur GN, Zmijewski JW, et al. Direct, activating interaction between glycogen synthase kinase-3beta and p53 after DNA damage. Proc Natl Acad Sci USA. 2002; 99:7951–5. [PubMed: 12048243]

64. Chen Z, Trotman LC, Shaffer D, et al. Crucial role of p53-dependent cellular senescence in suppression of Pten-deficient tumorigenesis. Nature. 2005; 436:725–30. [PubMed: 16079851]

65. Collado M, Serrano M. Senescence in tumours: evidence from mice and humans. Nat Rev Cancer. 2010; 10:51–7. [PubMed: 20029423]

66. Valkenburg KC, Hostetter G, Williams BO. Concurrent Hepsin overexpression and adenomatous polyposis coli deletion causes invasive prostate carcinoma in mice. Prostate. 2015; 75:1579–85. [PubMed: 26139199]

67. Anderson PD, McKissic SA, Logan M, et al. Nkx3.1 and Myc crossregulate shared target genes in mouse and human prostate tumorigenesis. J Clin Invest. 2012; 122:1907–19. [PubMed: 22484818]

68. Klezovitch O, Chevillet J, Mirosevich J, et al. Hepsin promotes prostate cancer progression and metastasis. Cancer Cell. 2004; 6:185–95. [PubMed: 15324701]

Europe PMC Funders Author Manuscripts

Europe PMC Funders Author Manuscripts

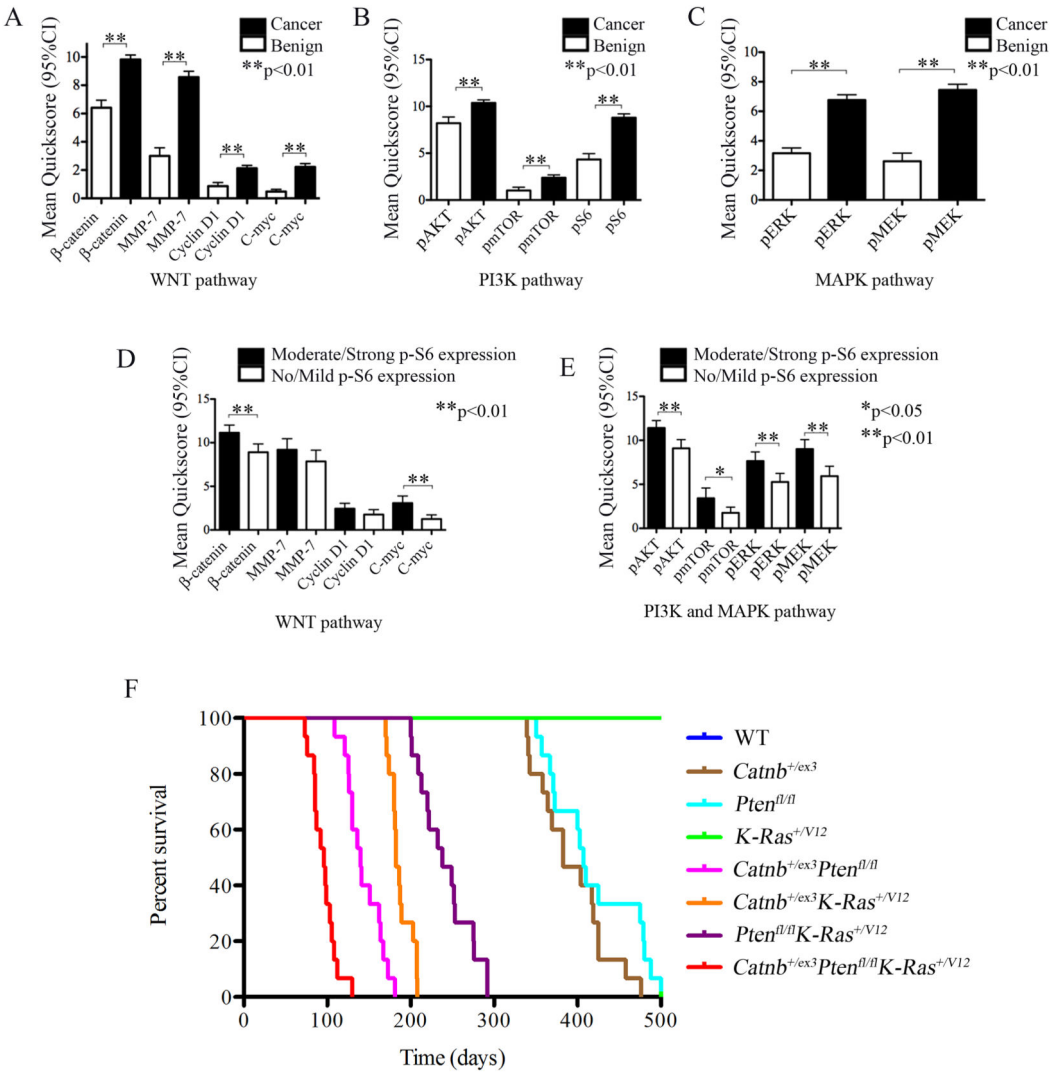

	WT	*Pten* $^{fl/fl}$	*Catn* $^{+/ex3}$	*K-Ras* $^{+/V12}$	*Catn* $^{+/ex3}$ *K-Ras* $^{+/V12}$	*Pten* $^{fl/fl}$ *K-Ras* $^{+/V12}$	*Catn* $^{+/ex3}$ *Pten* $^{fl/fl}$
Pten $^{fl/fl}$	p<0.0001						
Catn $^{+/ex3}$	p<0.0001	p<0.0001					
K-Ras $^{+/V12}$	N.S. (p=1)	N.S. (p=0.104)	p<0.0001				
Catn $^{+/ex3}$ *K-Ras* $^{+/V12}$	p<0.0001	p<0.0001	p<0.0001	p<0.0001			
Pten $^{fl/fl}$ *K-Ras* $^{+/V12}$	p<0.0001	p<0.0001	p<0.0001	p<0.0001	p<0.0001		
Catn $^{+/ex3}$ *Pten* $^{fl/fl}$	p<0.0001	p<0.0001	p<0.0001	p<0.0001	p<0.0001	p<0.0001	
Catn $^{+/ex3}$ *Pten* $^{fl/fl}$ *K-Ras* $^{+/V12}$	p<0.0001	p<0.0001	p<0.0001	p<0.0001	p<0.0001	p<0.0001	p<0.0001

Figure 1. Immunohistochemistry for WNT, PI3K, MAPK and mTOR pathway markers in a human prostate cancer tissue-micro-array (TMA) and Kaplan-Meier survival curves for *in vivo* genetic models.

(A, B, C) Immunohistochemistry for expression of markers of WNT (A), PI3K (B) and MAPK (C) pathway activation in human PCa TMA demonstrating higher activity (as assessed by mean Quickscore) in cancer when compared to benign prostatic tissue. (D) Assessment of WNT pathway activation marker staining as a function of phospho-S6 staining (p-S6; no/mild versus moderate/strong staining, using mean Quickscore) demonstrating positive correlation of nuclear β-catenin and c-MYC with increased p-S6

staining. (E) Assessment of PI3K and MAPK pathway activation marker staining as function of p-S6 staining demonstrating positive correlation of all markers (p-AKT, p-MTOR, p-ERK and p-MEK) with increased p-S6 staining. Error bars = mean with 95% CI, Unpaired T test: *p<0.05, **p<0.01. (F) Kaplan-Meier survival curves for mouse models (top) and statistical analysis (bottom). The median survival for triple mutant (*Pb-Cre4*$^{+}$ *Catnb*$^{+/ex3}$*Pten*$^{fl/fl}$ *K-Ras*$^{+/V12}$) mice was significantly lower than double mutants (p<0.0001, Log- Rank): 96 days (range 76-130), compared to 238 days (range 200-292), 182 days (range 170-208) and 140 days (range 109-181) for the double mutants: *Pb-Cre4*$^{+}$ *Pten*$^{fl/fl}$ *K-Ras*$^{+/V12}$, *Pb-Cre4*$^{+}$ *Catnb*$^{+/ex3}$ *K-Ras*$^{+/V12}$ and *Pb-Cre4*$^{+}$ *Catnb*$^{+/ex3}$*Pten*$^{fl/fl}$, respectively. All double mutant combinations had a significantly shorter survival when compared to single mutants (p<0.0001, Log-Rank). The survival of *Pb-Cre4*$^{+}$ *Catnb*$^{+/ex3}$ and *Pb-Cre4*$^{+}$ *Pten*$^{fl/fl}$ was 383 days (range 339-476) and 407 (range 350-479), respectively. *Pb-Cre4*$^{+}$ *K-Ras*$^{+/V12}$ and wild-type mice all survived to the end-point of the experiment (500 days). Wild-type (WT), *Catnb*$^{+/ex3}$ (β-catenin).

Europe PMC Funders Author Manuscripts

Europe PMC Funders Author Manuscripts

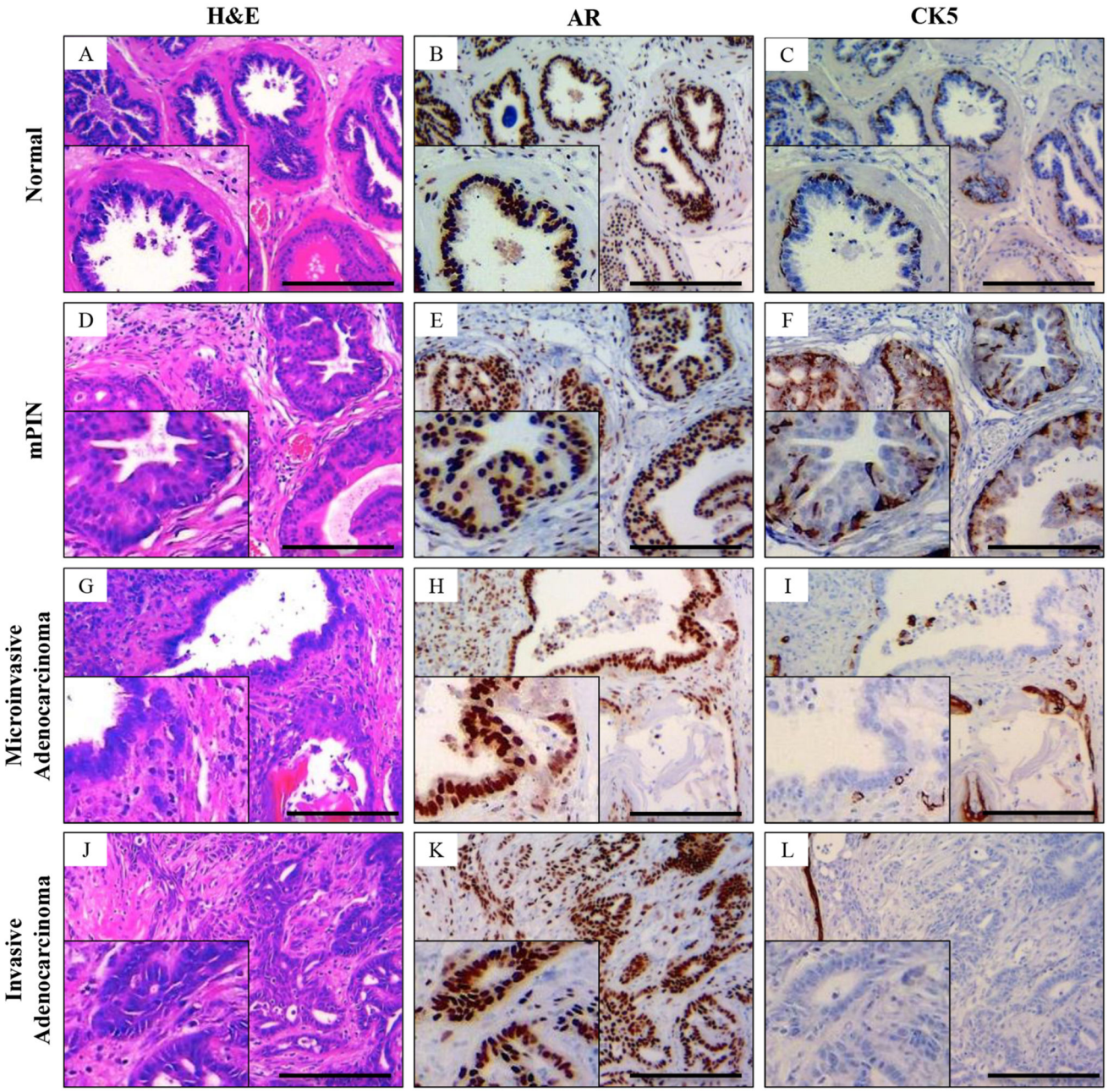

Figure 2. Histological characterisation of normal, mouse prostate intraepithelial neoplasia (mPIN), microinvasive adenocarcinoma and diffuse adenocarcinoma of the mouse prostate.

(A) Hematoxylin and eosin (H&E) staining of the histologically normal prostate gland. (B) Androgen receptor (AR) immunohistochemistry demonstrates avid staining of the luminal cells with (C) cytokeratin (CK) 5 staining the membrane of the basal layer abutting the basement membrane in a continuous fashion. (D) mPIN has a characteristic appearance with increased cell proliferation within the glands with frequent cellular atypia. (E,F) mPIN lesions display widespread AR staining (E) while the CK5 staining remains continuous (F). (G) In microinvasive adenocarcinoma, the glandular structure begins distort with focal areas

of microinvasion of AR positive (H) epithelial cells into the surrounding stroma. (I) At the site of invasion there is loss of the continuous CK5 staining basal layer. (J) H&E staining of prostate adenocarcinoma sections demonstrate diffuse invasion of epithelial cells into the stroma, with fusion of glands and areas of cribriform pattern, which is pathognomonic of human Gleason pattern 4. (K) AR staining demonstrates intensely stained epithelial cells invading the stroma with loss of the basal marker CK5 (L). Bars = 200 μm. Insets magnified two times.

Europe PMC Funders Author Manuscripts

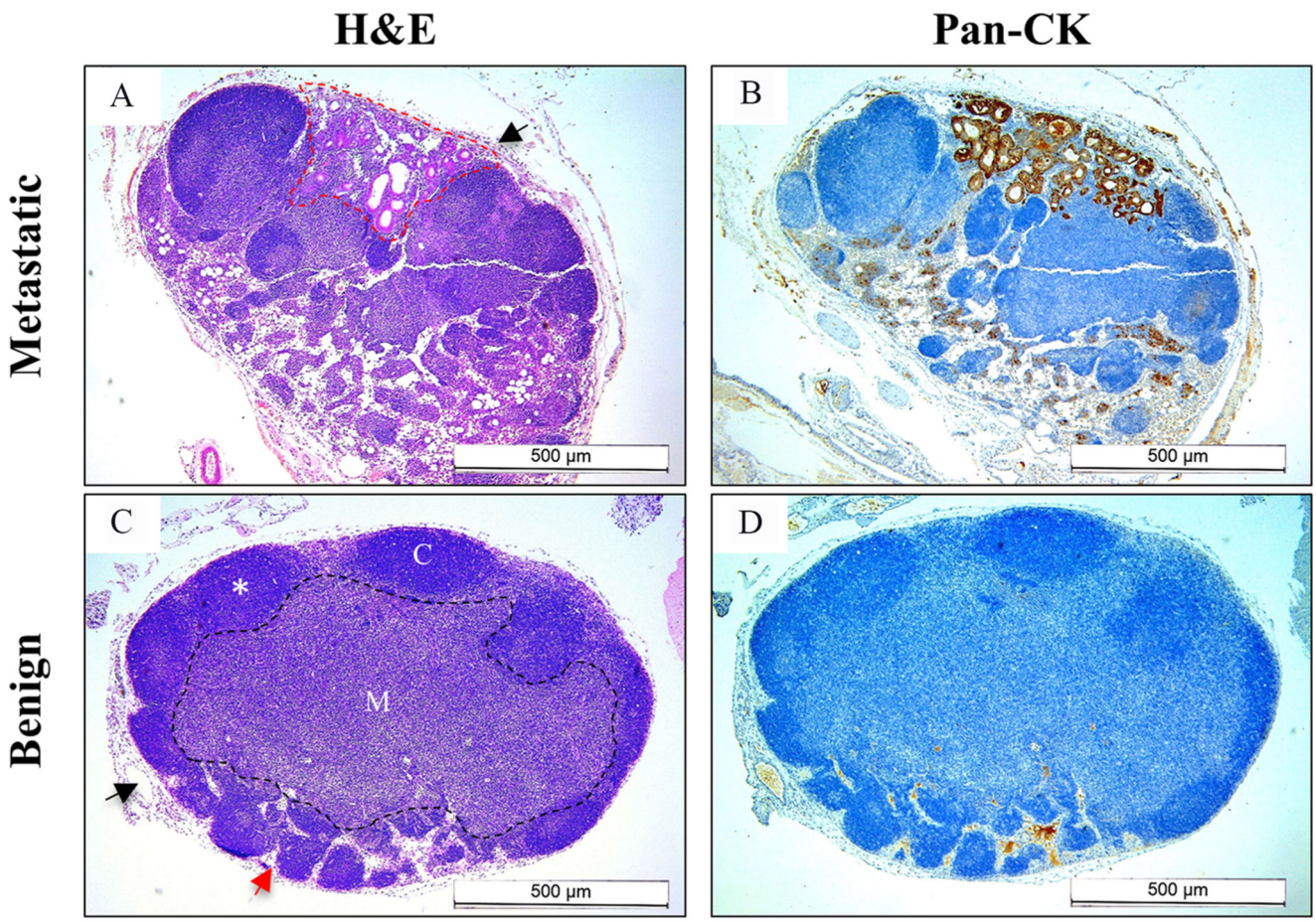

Figure 3. Lymph node characterisation.

(A) Metastatic prostate epithelium extending from the capsule (black arrow) and infiltrating into the node (red-dotted line). (B) Metastatic node staining avidly for pan-cytokeratin. (C) Benign reactive node with the inner medulla (M) and outer cortex (C) separated by the dotted black line. The capsule and marginal sinus (black arrow) surrounds the node with the cortex separated by cortical sinuses (red arrow). Germinal center within the cortex of the node (*). (D) Minimal non-specific pan-cytokeratin staining in a benign node. Scale bars as indicated.

Europe PMC Funders Author Manuscripts

Europe PMC Funders Author Manuscripts

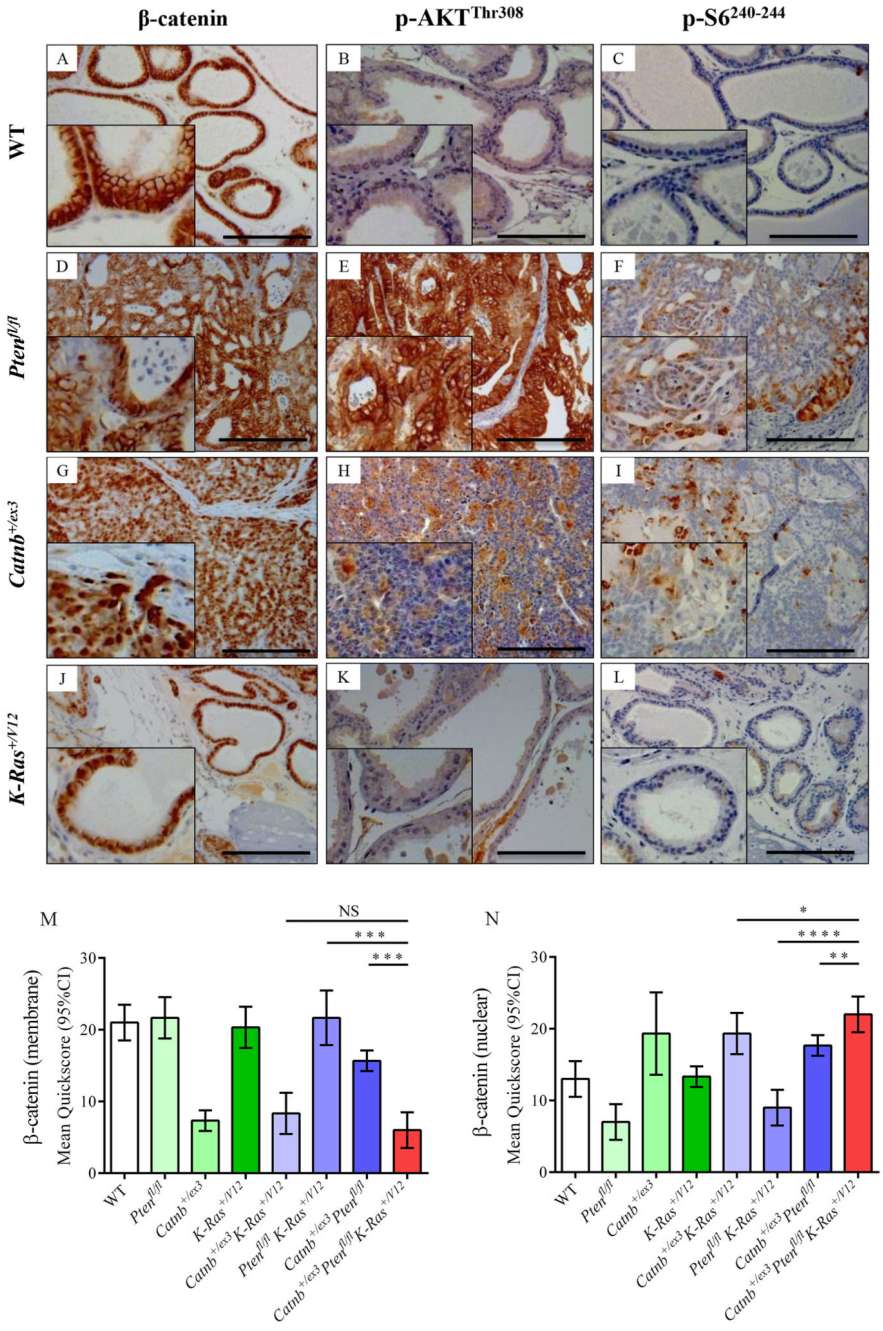

Figure 4. Immunohistochemistry for β-catenin, p-AKT^{Thr308} and p-S6$^{240-244}$ in wild type and single allele mouse models.

(A-L) Immunostaining using antibodies against β-catenin (A, D, G, J), p-AKT^{Thr308} (B, E, H, K), and p-S6$^{240-244}$ (C, F, I, L) on *WT* (A-C), *Pb-Cre4*$^{+}$ *Pten*$^{fl/fl}$ (D-F), *Pb-Cre4*$^{+}$ *Catnb* $^{+/ex3}$(G-I) and *Pb-Cre4*$^{+}$ *K-Ras*$^{+/V12}$ (J-I) cohorts of mice (n=4) at the endpoint of the experiment (500 days or when sick). Bars = 200 μm. Insets magnified two times. (M, N) Quickscore quantification of β-catenin membrane-specific (M) and nuclear staining (N) in all genotypes, including staining presented in Fig.5. Note Quickscore quantitation of p-AKT^{Thr308} and p-S6$^{240-244}$ for all genotypes is presented in Fig.5M and N. For clarity,

significance of Quickscore staining in triple mutant vs double mutant cohorts only is presented on the graphs (NS, not significant;* P<0.05; ** P<0.01; *** P<0.001; unpaired two-tailed t-test, n=4); full statistical comparisons of all genotypes are given in Supplementary Table 1. WT prostates demonstrated predominantly membranous staining for β-catenin, with some nuclear staining, but no p-AKT^{Thr308} or p-S6$^{240-244}$ reactivity (A-C). *Pten*$^{fl/fl}$ tumours had membrane staining for β-catenin, rare nuclear positivity, diffuse staining for p-AKT^{Thr308} and focal staining for p-S6$^{240-244}$ (D-F). *Catnb*$^{+/ex3}$ tumours had strong nuclear staining of β-catenin, with reduced cell membrane staining, and focal positive staining for p-AKT^{Thr308} and p-S6$^{240-244}$ (G-I). *K-Ras*$^{+/V12}$ samples had predominantly membrane staining for β-catenin with some nuclear positivity and no staining for p-AKT^{Thr308} or p-S6$^{240-244}$ (J-L).

Europe PMC Funders Author Manuscripts

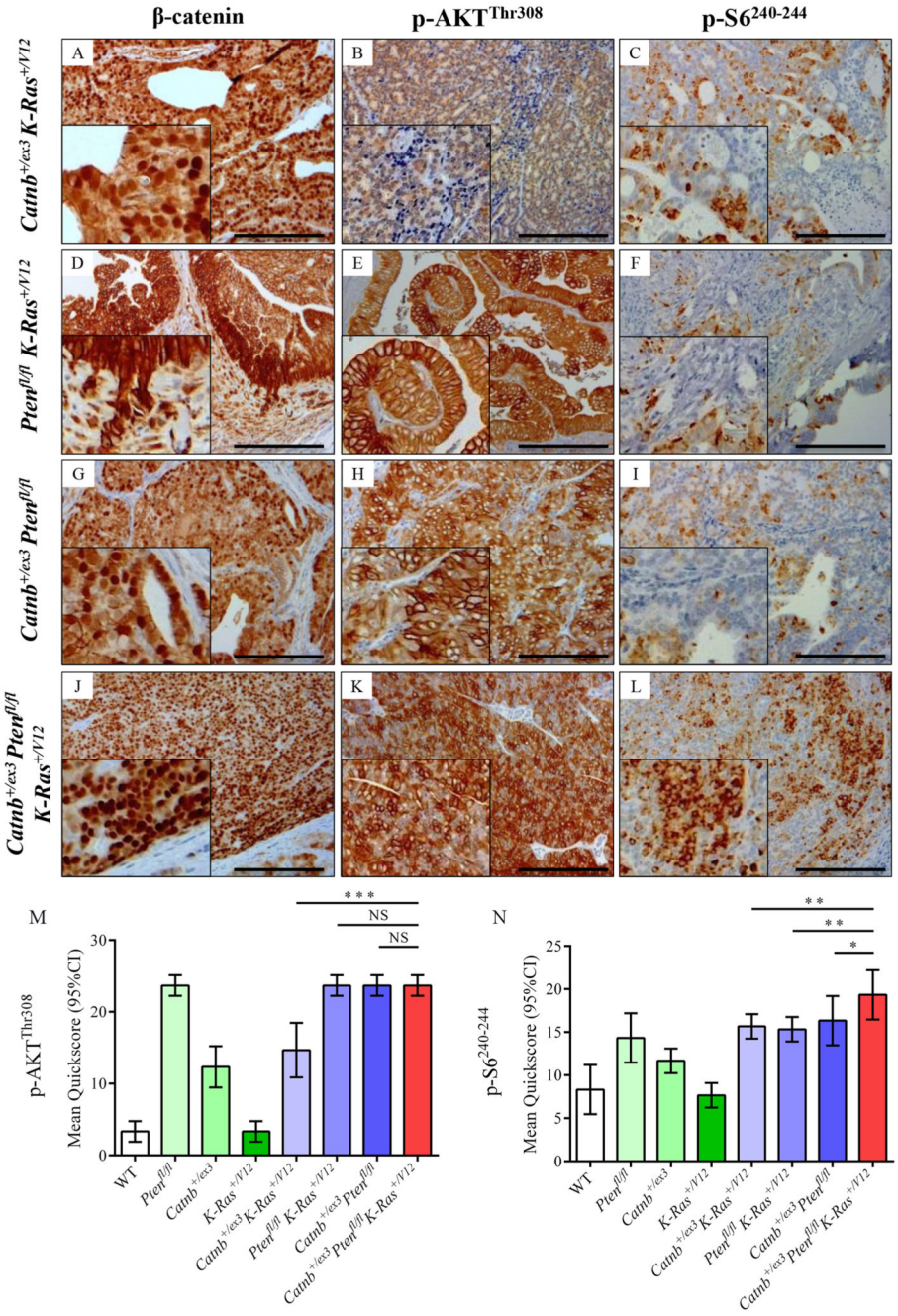

Figure 5. Immunohistochemistry for β-catenin, p-AKT^{Thr308} and p-S6$^{240-244}$ in double and triple allele mouse models.

(A-L) Immunostaining for β-catenin (A, D, G, J), p-AKT^{Thr308} (B, E, H, K), and p-S6$^{240-244}$ (C, F, I, L) on *Pb-Cre4*$^{+}$ *Catnb*$^{+/ex3}$ *K-Ras*$^{+/V12}$ (A-C), *Pb-Cre4*$^{+}$ *Pten*$^{fl/fl}$ *K-Ras*$^{+/V12}$ (D-F), *Pb-Cre4*$^{+}$ *Catnb*$^{+/ex3}$*Pten*$^{fl/fl}$ (G-I) and *Pb-Cre4*$^{+}$ *Catnb*$^{+/ex3}$*Pten*$^{fl/fl}$*K-Ras*$^{+/V12}$ (J-L) cohorts of mice (n=4) at the endpoint of the experiment (500 days or when sick. Bars = 200 μm. Insets magnified two times. (M, N) Quickscore quantification of p-AKT^{Thr308} and p-S6$^{240-244}$ for all genotypes. For Quickscore quantification of β-catenin membrane-specific (M) and nuclear staining (N), see Fig.4M,N. For clarity, significance of Quickscore staining

in triple mutant vs double mutant cohorts only is presented on the graphs (NS, not significant;* P<0.05; ** P<0.01; *** P<0.001; unpaired two-tailed t-test, n=4); full statistical comparisons of all genotypes are given in Supplementary Table 1. *Catnb*$^{+/ex3}$*K-Ras*$^{+/V12}$ tumours demonstrated predominantly nuclear staining of β-catenin, with weak focal staining for p-AKT^{Thr308} and p-S6$^{240-244}$ (A-C). *Pten*$^{fl/fl}$ *K-Ras*$^{+/V12}$ tumours had strong membrane staining for β-catenin, strong diffuse staining for p-AKT^{Thr308} and focal positive staining for p-S6$^{240-244}$ (D-F). *Catnb*$^{+/ex3}$*Pten*$^{fl/fl}$ tumours demonstrated both nuclear and membrane-specific β-catenin staining, diffuse staining for p-AKT^{Thr308} and focal positive staining for p-S6$^{240-244}$ (G-I). *Catnb*$^{+/ex3}$*Pten*$^{fl/fl}$*K-Ras*$^{+/V12}$ tumours stained avidly for nuclear β-catenin with diffuse strong staining for both p-AKT^{Thr308} and p-S6$^{240-244}$ (J-L), the latter being significantly higher than in all other cohorts.

Europe PMC Funders Author Manuscripts

Europe PMC Funders Author Manuscripts

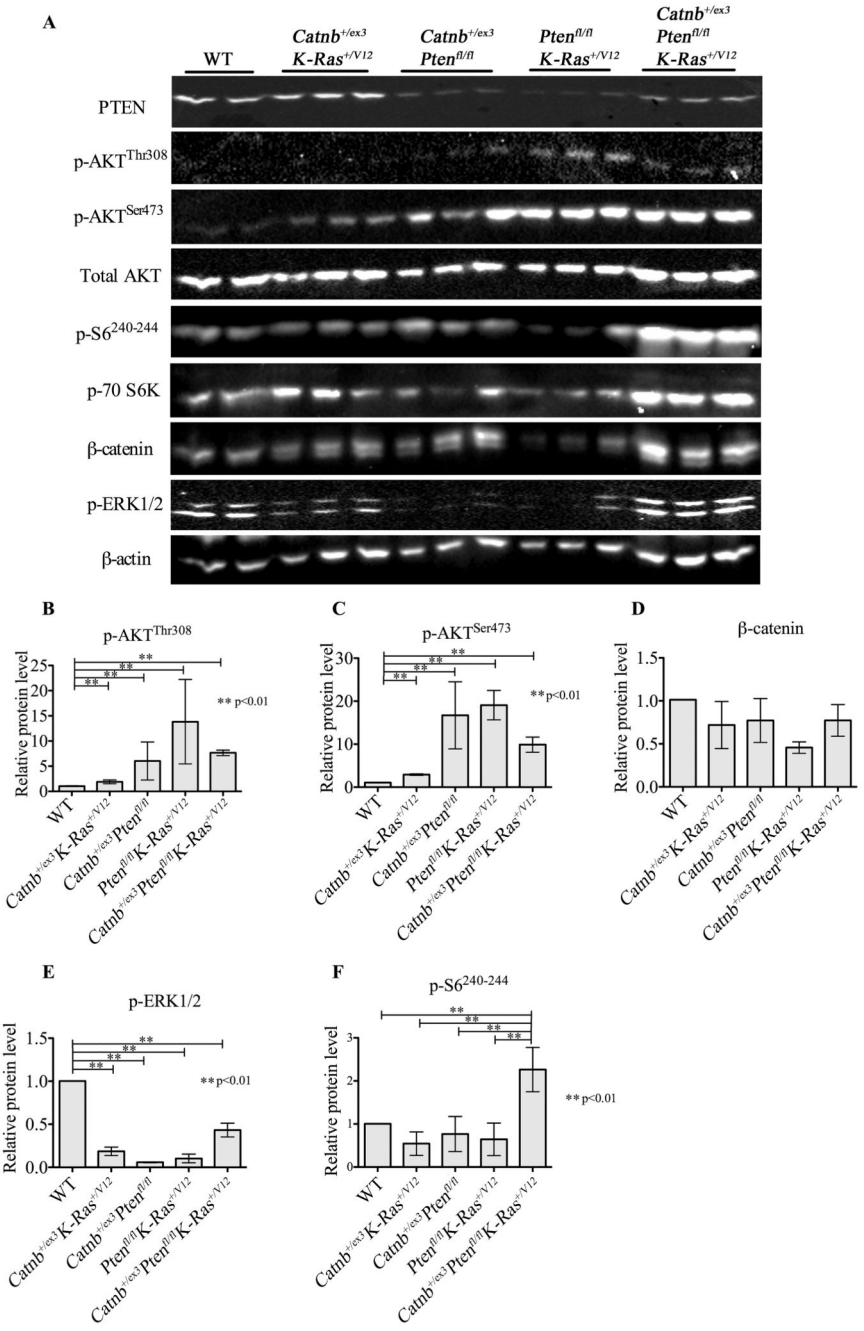

Figure 6. Biochemical analysis of signalling pathways in prostate tissue from double and triple allele models.

(A) Western-blot analysis of markers of activation of the PI3K, WNT, MAPK and mTOR signalling pathways for Wild-type (WT), double (*Catnb*$^{+/ex3}$*K-Ras*$^{+/V12}$, *Pten*$^{fl/fl}$*Catnb*$^{+/ex3}$ and *Pten*$^{fl/fl}$*K-Ras*$^{+/V12}$) and triple (*Catnb*$^{+/ex3}$*Pten*$^{fl/fl}$*K-Ras*$^{+/V12}$) mutants. Protein was extracted from fresh frozen prostate tissue from 100-day old mice for each cohort (n=3). The following antibodies were used: PI3K pathway markers, PTEN, p-AKT^{Thr308}, p-AKT^{Ser473} and total AKT; WNT pathway marker, β-catenin; MAPK pathway marker, pERK1/2; mTOR pathway markers, p70S6K and pS6$^{240/244}$. β-actin was used as a loading reference. (B–F)

Relative quantitation of p-AKT^{Thr308} (B), pAKT^{Ser473} (C), β-catenin (D), p-ERK1/2 (E) and p-S6$^{240/244}$ (F). Error bars = mean with 95% CI, *p<0.05, **p<0.01, unpaired two-tailed t test, n=3.

Europe PMC Funders Author Manuscripts